Coatings **2015**, *5*, 357-365; doi:10.3390/coatings5030357

OPEN ACCESS

coatings

ISSN 2079-6412

www.mdpi.com/journal/coatings

Article

Biofouling Prevention of Ancient Brick Surfaces by TiO_2-Based Nano-Coatings

Lorenzo Graziani and Marco D'Orazio *

Department of Construction, Civil Engineering and Architecture (DICEA), Università Politecnica delle Marche, via Brecce Bianche, 60131 Ancona, Italy; E-Mail: l.graziani@univpm.it

* Author to whom correspondence should be addressed; E-Mail: m.dorazio@univpm.it; Tel./Fax: +39-071-220-4587.

Academic Editor: Enrico Quagliarini

Received: 27 April 2015 / Accepted: 22 July 2015 / Published: 28 July 2015

Abstract: Brick constitutes a significant part of the construction materials used in historic buildings around the world. This material was used in Architectural Heritage for structural scope, and even for building envelopes. Thus, components made of clay brick were subjected to weathering for a long time, and this causes their deterioration. One of the most important causes for deterioration is biodeterioration caused by algae and cyanobacteria. It compromises the aesthetical properties, and, at a later stage, the integrity of the elements. In fact, traditional products used for the remediation/prevention of biofouling do not ensure long-term protection, and they need re-application over time. The use of nanotechnology, especially the use of photocatalytic products for the prevention of organic contamination of building façades is increasing. In this study, TiO_2-based photocatalytic nano-coatings were applied to ancient brick, and its efficiency towards biofouling was studied. A composed suspension of algae and cyanobacteria was sprinkled on the bricks' surface for a duration of twelve weeks. Digital Image Analysis and colorimetric measurements were carried out to evaluate algal growth on specimens' surfaces. Results show that photocatalytic nano-coating was able to inhibit biofouling on bricks' surfaces. In addition, substrata (their porosity and roughness) clearly influences the adhesion of algal cells.

Keywords: biofouling; brick; façades; nanotechnology; nanocoating; algae; cyanobacteria; cultural heritage; TiO_2; photocatalysis

1. Introduction

Fired clay bricks were used in masonry, roofing, cladding and ornamentation as a building material from antiquity, and it has been used throughout history until the present. Buildings and monuments with fired clay elements, whether in the form of bricks, wall and roofing tiles or floor tiles can be found throughout the world. A significant number of the architectural elements built with this material are part of our cultural heritage and, therefore, ought to be preserved since they have historical and artistic value.

Biodeterioration of architectural elements may results from their exposure to soil, water, wastewater, and waste products. When architectural materials are exposed to favourable conditions of light, temperature and moisture, the adhesion and growth of algae and cyanobacteria occurs (e.g., *Chlorella mirabilis* and *Chroococcidiopsis fissurarum*) [1,2], thus, leading to the occurrence of large amounts of biological matter [3]. The result is obviously in deterioration of appearance, but also in the performance and functionality of buildings and structures as they can become compromised. The importance of studying biofouling of building stone (both natural and man-made stones) led to the publication of many research paper and review articles [4–7].

Actually, traditional products used for remediation/prevention of biofouling do not ensure long-term protection, and they need re-application over time, increasing maintenance costs [8,9]. Thus, special attention must be drawn to the prevention of biodeterioration of stone, concrete, bricks and mortar.

In this direction, self-cleaning and biocide coatings could improve the preservation of ancient and historical surfaces, both from the point of view of the maintenance of their original aesthetic aspect and in easier removal of external degrading agents, limiting cleaning and conservation actions, and, thus, reducing costs [10–22]. The state-of-the-art shows a limited nano-functionalization of elements made with materials used in the field of Architectural and the Archaeological Heritage.

In this study, the biofouling process on clay brick specimens was investigated and correlations between the properties of substrate and the bioreceptivity of material were found. In addition, the anti-biofouling efficiency of titanium dioxide (TiO_2) was investigated by comparing nano-engineered bricks with original ones.

2. Experimental Section

2.1. Samples Preparation and Characterization

Twelve prismatic ($80 \times 80 \times 30$ mm^3) specimens were manually mixed and formed. After drying of the specimens, they were fired at 700 °C because this temperature allows the re-production of clay bricks with similar characteristics to ancient clay bricks, as previously tested [23–26]. Table 1 shows tested specimens and their characteristics.

In order to evaluate the influence of surface roughness on the biofouling process, six specimens were manually smoothed (S) with sand paper, while the other six were left in their original (R) state. For each subgroup, three specimens were coated with a 1% (w/v) of TiO_2 nanocoating aqueous solution, and three specimens remained uncoated and were, hence, used as control.

Total porosity and porous distribution of the clay brick specimens were measured onto five samples by mercury intrusion porosimeter (Micromeritics Autopore III). Porosimetry tests were conducted according to the ASTM D4404–10 standard [27], while average surface roughness parameters (R_a) were

evaluated according to European standards [28,29] by using a Diavite DH-5 rugosimeter of a length of 1.34 cm, with a cut-off length of 0.8 mm.

Since biofouling causes aesthetical variation, mainly color variation, the original color of the specimens was measured by a CM2600d colorimeter (Konika Minolta Inc., Milan, Italy), using a daylight illuminant (D65) and a 10° observer angle [30].

2.2. Nano-Coating Application and Accelerated Growth Test

TiO_2 sol was composed of very fine anatase crystals with a crystallite size of 4 nm, as estimated by the elaboration of XRD patterns (Figure 1).

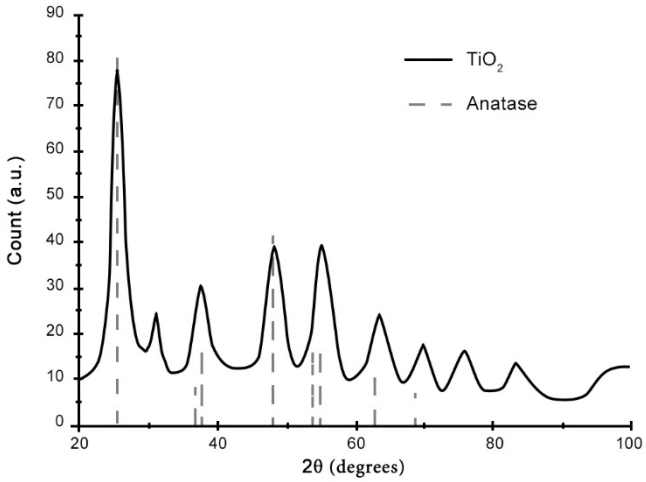

Figure 1. XRD pattern of TiO_2 solution.

The solution (2 mL) was manually applied on fired clay bricks (after thermal treatment) with an air spray gun, with a nozzle of 0.8 mm diameter at a distance of approximately 250 mm. This deposition method allows the replication of a real, *in situ* application.

In order to perform the accelerated growth test, a water run-off test was carried out (for 12 weeks) inside a glass chamber in which specimens were positioned on two aluminum racks, front-to-front along the long dimensions of the chamber (scheme in Figure 2).

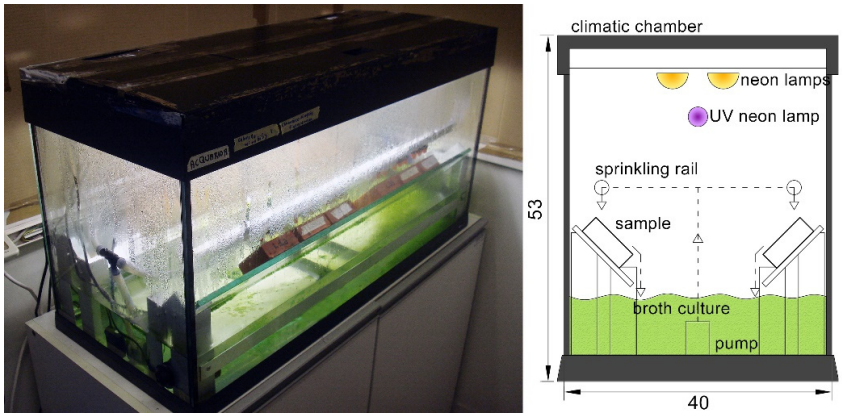

(**a**) (**b**)

Figure 2. View (**a**) and schematic view (**b**) of test apparatus.

Two test strains (*Chlorella mirabilis* and *Chroococcidiopsis fissurarum*) were selected for use in the accelerated growth tests, since they are typically found on building façades [2].

Microalgae suspensions were inoculated at a concentration of 5% (v/v) into the chamber, containing forty liters of Bold's Basal Medium (BBM). In order to maintain the ideal growth conditions inside the chamber, the temperature of the broth culture was maintained at about 24 °C with a heater (Heather Bluclima 150 W) and daylight was provided by two 39 W neon lamps (Sylvania, model TopLife, Milan, Italy) with a light temperature of 500 K.

The samples were irradiated with an average UV intensity of 8 W/m^2, provided by the two UV lamps (model TL-D Blacklight Blue 18 W, wavelength of 365 nm, Philips, Monza, Italy), which were placed on the lid of the chamber at the same distance from the two racks. During the light period of 14 h, both solar light and UV-A lamps were switched on, while for the remaining 10 h, all the lamps were turned off to simulate the night period.

The broth culture inside each glass chamber was sprinkled over the top of the specimens by two PVC tubes, joined to a pump, with a run/off cycle of 15 min, for a duration of 6 h (3 h run and 3 h off).

2.3. Evaluation of Biofouling on the Specimens

Two different techniques were used to evaluate the biofouling process on specimens' surfaces. Colorimetric analysis was used to evaluate the color variation during time, and Digital Image Analysis (DIA) of scanned images of the samples was used to measure the extension of algal coverage. Both quantitative analyses were carried out weekly during the duration of the accelerated growth test.

Color measurements were performed by using the same method described in Section 2.1, and color variation was calculated with well noted equation (Equation (1)).

$$\Delta E = \sqrt{(L_0^* - L_t^*)^2 + (a_0^* - a_t^*)^2 + (b_0^* - b_t^*)^2} \quad (1)$$

where L_0^*, a_0^* and b_0^* are the CIELab coordinates of untreated samples (time zero) and L_t^*, a_t^* and b_t^* are the CIELab coordinates of the sample at each measuring time.

At the same time, the surfaces of specimens were digitized weekly by an office scanner at a resolution of 600 dpi. Acquired images were manipulated with a high-pass filter (threshold) to exclude the uncontaminated parts. Obtained images were binarized and only pixels contaminated by microalgae were counted. Extent of algal coverage was evaluated by ImageJ [31,32] software that was able to return the percentage (0% = uncontaminated, 100% = completely contaminated) of area covered by microorganisms.

In order to avoid the influence of other changes in the material, specimens were dried for two hours before each measurement. In this way, color variation can be only associated to the growth of algal cells.

3. Results and Discussion

3.1. Material Characterization

Table 1 shows main parameters measured to characterize the material tested in this paper.

TiO_2 nano-film caused no significant color variation, indeed, the values of color coordinates L^*, a^* and b^* of the treated specimens are very close to the values of the untreated ones. This first finding is

very important because it means the application of TiO_2 sol is compatible with ancient buildings of cultural heritage.

Table 1. Tested clay brick specimens with physical characteristics (mean value ± standard deviation). Each sample is representative of three specimens.

Sample	Treatment	Total Porosity (%)	Roughness R_a (μm)	*L**	*a**	*b**
RU	Untreated	36.65 ± 0.65	8.9 ± 0.9	62.42 ± 1.70	11.61 ± 1.32	19.39 ± 1.21
RT	TiO_2		8.1 ± 0.4	62.30 ± 1.72	12.40 ± 0.99	19.84 ± 1.13
SU	Untreated		1.11 ± 0.04	59.51 ± 2.49	14.65 ± 0.91	22.99 ± 1.09
ST	TiO_2		1.6 ± 0.2	60.94 ± 2.75	13.59 ± 0.47	20.61 ± 0.80

Figure 3 shows the difference between the profile of an original rough specimen and a smoothed one. In the first case, many asperities are visible in the image, while no asperity (or very few) is visible on the profile of smoothed specimen. Figure 4 shows deposition of nano-TiO_2 crystals on a treated specimen. The average particle size, after TiO_2 deposition, is around 40–50 nm, as shown in Figure 4.

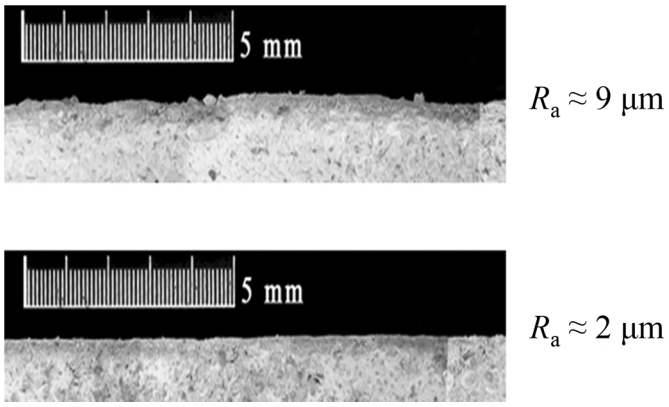

Figure 3. Magnification of specimens' profile. Rough surface above and smooth surface bottom.

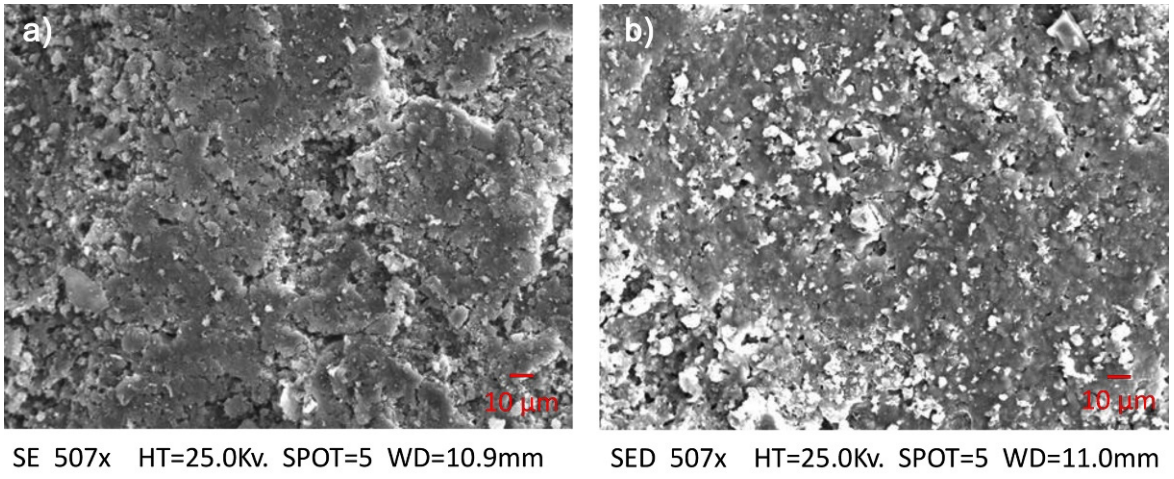

Figure 4. SEM observation of untreated (**a**) and treated brick specimens (**b**). White spots represent TiO_2 crystals.

3.2. Results of Biofouling

Figure 5 shows the variation of biofouling during time, expressed as color variation and percentage of area covered by algal cells. Since color measurement and DIA can be considered as two complementary techniques [11,21] (as visible in Figure 5), discussion of the results will focus on the extent of algal coverage (Figure 5b).

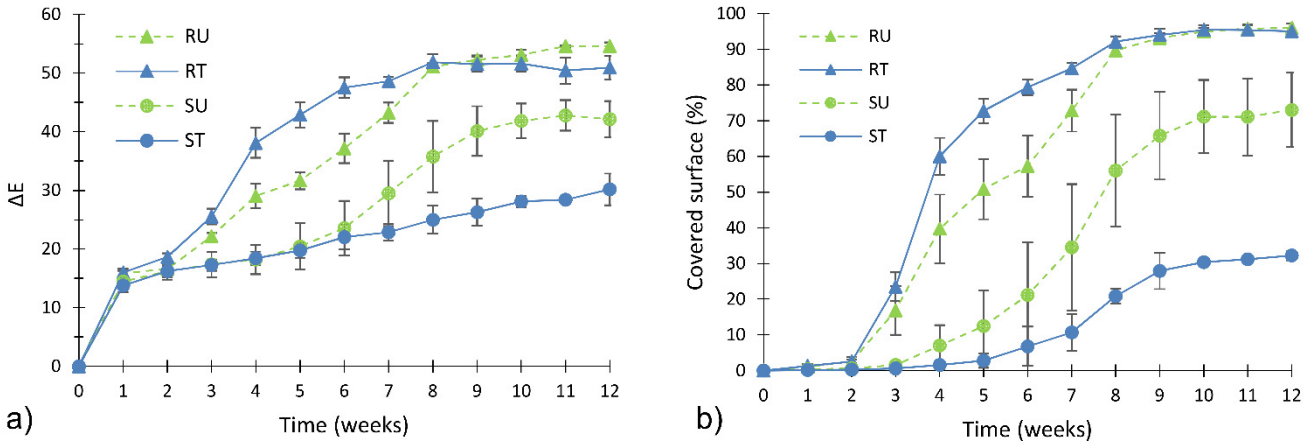

Figure 5. Extent of algal fouling evaluated by colorimetric analysis (**a**) and DIA (**b**) during the accelerated fouling test.

By considering untreated specimens, it is possible to find a correlation between biofouling and the intrinsic characteristics of clay bricks. Biofouling on smoothed specimens (SU) was slower than that on rough specimens (RU). Algal coverage on the RU specimens reached 96% at the end of accelerated growth test, while it reached 73% in the case of the SU specimens. Thus, by reducing surface roughness, from about 8 µm to about 1 µm, algal coverage was reduced by more than 20%.

The effect of TiO_2 treatment was studied by comparing the RU-RT curve and the SU-ST curve. Figure 5b shows that the trend of treated smooth specimens' ST is always lower than trend of untreated smooth specimens' SU. In detail, the application of TiO_2 nanoparticles allowed a reduction of algal coverage of about 40% (SU-ST) at the end of the accelerated biofouling test.

The efficiency of TiO_2 nanofilm was not confirmed in case of roughness RT specimens, which show a very similar trend to that of the corresponding un-treated specimens (RU). This latter finding was caused by the synergic effect of porosity and roughness. Indeed, porosity was able to enhance the water (and nutrient) retention into the substrata, while roughness offers many asperities, where algal cells can anchor. Thus, rough specimens promote the adhesion and anchorage of algal cells better than smoothed specimens.

4. Conclusions

In this study, the correlation between intrinsic characteristics of clay brick and biofouling were investigated. In addition, the anti-biofouling efficiency of TiO_2 was studied in order to improve the preservation of ancient and historical brick surfaces in regards to the maintenance of their original aesthetic aspect, limiting cleaning and conservation actions, and, thus, reducing costs.

The accelerated laboratory growth test performed in this study, and the methods used to collect data, were confirmed to be adequate enough to study biological fouling on ancient brick surfaces. Moreover, colorimetric analysis and DIA could be used in combination, being complementary. The influence of roughness and porosity play a key role in the biofouling process, and the TiO_2 nanocoating treatment was proved to inhibit the biofouling of clay bricks irradiated with UV-A light, except in the case of the roughness of specimens. In the case of rough specimens, the high number of superficial asperities proved to promote the adherence of microalgae to the substratum, thus increasing the colonization rate and, hence, leading to a rapid coverage of the nanofilm, which could no longer be activated by UV light. Further research to optimize the TiO_2 efficiency under the experimental conditions assayed are underway.

Acknowledgments

The authors wish to thank Salentec S.r.l. for the supply of nanostructured TiO_2 solutions. The authors also wish to thank the researchers of Department of Agricultural, Food and Enviromental Sciences (D3A) from Università Politecnica delle Marche (Italy) for their contribution in the biological growth of algae microcultures.

Author Contributions

L. Graziani and M. D'Orazio conceived and designed the experiments; L. Graziani performed the experiments; L. Graziani analyzed the data; L. Graziani and M. D'Orazio wrote the paper.

Conflicts of Interest

The authors declare no conflict of interest.

References

1. Barberousse, H.; Lombardo, R.J.; Tell, G.; Coute, A. Factors involved in the colonisation of building facades by algae and cyanobacteria in France. *Biofouling* **2006**, *22*, 69–77.
2. Barberousse, H.; Ruot, B.; Yéprémian, C.; Boulon, G. An assessment of façade coatings against colonisation by aerial algae and cyanobacteria. *Build. Environ.* **2007**, *42*, 2555–2561.
3. Tran, T.H.; Govin, A.; Guyonnet, R.; Grosseau, P.; Lors, C.; Garcia-Diaz, E.; Damidotb, D.; Devèse, O.; Ruot, B. Influence of the intrinsic characteristics of mortars on biofouling by *Klebsormidium flaccidum*. *Int. Biodeterior. Biodegrad.* **2012**, *70*, 31–39.
4. Warscheid, T.; Braams, J. Biodeterioration of stone : A review. *Int. Biodeterior. Biodegrad.* **2001**, *46*, 343–368.
5. Gaylarde, C.; Ribas Silva, M.; Warscheid, T. Microbial impact on building materials: An overview. *Mater. Struct.* **2003**, *36*, 342–352.
6. Miller, A.Z.; Sanmartin, P.; Pereira-Pardo, L.; Dionisio, A.; Saiz-Jimenez, C.; Macedo, M.F.; Prieto, B. Bioreceptivity of building stones: A review. *Sci. Total Environ.* **2012**, *426*, 1–12.
7. Coutinho, M.L.; Miller, A.Z.; Macedo, M.F. Biological colonization and biodeterioration of architectural ceramic materials: An overview. *J. Cult. Herit.* **2015**, in Press.

8. Tiano, P. Biodegradation of Cultural Heritage: Decay Mechanisms and Control Methods. Available online: http://www.arcchip.cz/w09/w09_tiano.pdf (accessed on 20 July 2015).
9. Roy, S.K.; Thye, L.B.; Northwood, D.O. The evaluation of paint performance for exterior applications in Singapore's tropical environment. *Build. Environ.* **1996**, *31*, 477–486.
10. Fonseca, A.J.; Pina, F.; Macedo, M.F.; Leal, N.; Romanowska-Deskins, A.; Laiz, L.; Gómez-Bolea, A.; Saiz-Jimenez, C. Anatase as an alternative application for preventing biodeterioration of mortars: Evaluation and comparison with other biocides. *Int. Biodeterior. Biodegrad.* **2010**, *64*, 388–396.
11. Graziani, L.; Quagliarini, E.; Osimani, A.; Aquilanti, L.; Clementi, F.; Yéprémian, C.; Lariccia, V.; Amoroso, S.; D'Orazio, M. Evaluation of inhibitory effect of TiO_2 nanocoatings against microalgal growth on clay brick façades under weak UV exposure conditions. *Build. Environ.* **2013**, *64*, 38–45.
12. Graziani, L.; Quagliarini, E.; Osimani, A.; Aquilanti, L.; Clementi, F.; D'Orazio, M. The influence of clay brick substratum on the inhibitory efficiency of TiO_2 nanocoating against biofouling. *Build. Environ.* **2014**, *82*, 128–134.
13. Maury-Ramirez, A.; De Muynck, W.; Stevens, R.; Demeestere, K.; De Belie, N. Titanium dioxide based strategies to prevent algal fouling on cementitious materials. *Cem. Concr. Compos.* **2013**, *36*, 93–100.
14. Gladis, F.; Eggert, A.; Karsten, U.; Schumann, R. Prevention of biofilm growth on man-made surfaces: Evaluation of antialgal activity of two biocides and photocatalytic nanoparticles. *Biofouling* **2010**, *26*, 89–101.
15. La Russa, M.F.; Ruffolo, S.A.; Rovella, N.; Belfiore, C.M.; Palermo, A.M.; Guzzi, M.T.; Crisci, M. Multifunctional TiO_2 coatings for Cultural Heritage. *Prog. Org. Coat.* **2012**, *74*, 186–191.
16. MacMullen, J.; Radulovic, J.; Zhang, Z.; Dhakal, H.N.; Daniels, L.; Elford, J.; Leost, M.A.; Bennett, N. Masonry remediation and protection by aqueous silane/siloxane macroemulsions incorporating colloidal titanium dioxide and zinc oxide nanoparticulates: Mechanisms, performance and benefits. *Constr. Build. Mater*. **2013**, *49*, 93–100.
17. MacMullen, J.; Zhang, Z.; Dhakal, H.N.; Radulovic, J.; Karabela, A.; Tozzi, G.; Hannant, S.; Ali Alshehri, M.; Buhé, V.; Herodotou, C. Silver nanoparticulate enhanced aqueous silane/siloxane exterior facade emulsions and their efficacy against algae and cyanobacteria biofouling. *Int. Biodeterior. Biodegrad.* **2014**, *93*, 54–62.
18. MacMullen, J.; Zhang, Z.; Radulovic, J.; Herodotou, C.; Totomis, M.; Dhakal, H.N.; Bennett, N. Titanium dioxide and zinc oxide nano-particulate enhanced oil-in-water (O/W) facade emulsions for improved masonry thermal insulation and protection. *Energy Build.* **2012**, *52*, 86–92.
19. Martinez, T.; Bertron, A.; Escadeillas, G.; Ringot, E. Algal growth inhibition on cement mortar : Efficiency of water repellent and photocatalytic treatments under UV/VIS illumination. *Int. Biodeterior. Biodegrad.* **2014**, *89*, 115–125.
20. Radulovic, J.; MacMullen, J.; Zhang, Z.; Dhakal, H.N.; Hannant, S.; Daniels, L.; Elford, J.; Herodotou, C.; Totomis, M.; Bennett, N. Biofouling resistance and practical constraints of titanium dioxide nanoparticulate silane/siloxane exterior facade treatments. *Build. Environ.* **2013**, *68*, 150–158.
21. De Muynck, W.; Maury-Ramirez, A.; De Belie, N.; Verstraete, W. Evaluation of strategies to prevent algal fouling on white architectural and cellular concrete. *Int. Biodeterior. Biodegrad.* **2009**, *63*, 679–689.

22. Pinho, L.; Mosquera, M.J. Photocatalytic activity of TiO_2–SiO_2 nanocomposites applied to buildings: Influence of particle size and loading. *Appl. Catal. B Environ*. **2013**, *134–135*, 205–221.
23. Cardiano, P.; Ioppolo, S.; De Stefano, C.; Pettignano, A.; Sergi, S.; Piraino, P. Study and characterization of the ancient bricks of monastery of "San Filippo di Fragalà" in Frazzanò (Sicily). *Anal. Chim. Acta* **2004**, *519*, 103–111.
24. Lourenço, P.B.; Fernandes, F.M.; Castro, F. Handmade clay bricks: Chemical, physical and mechanical properties. *Int. J. Archit. Herit.* **2010**, *4*, 38–58.
25. Uğurlu Sağın, E.; Böke, H. Characteristics of bricks used in the domes of some historic bath buildings. *J. Cult. Herit.* **2013**, *14*, e73–e76.
26. Karaman, S.; Ersahin, S.; Gunal, H. Firing temperature and firing time influence on mechanical and physical properties of clay bricks. *J. Sci. Ind. Res.* **2006**, *65*, 153–159.
27. *ASTM D4404-10 Standard Test Method for Determination of Pore Volume and Pore Volume Distribution of Soil and Rock by Mercury Intrusion Porosimetry*; American Society for Testing and Materials: West Conshohocken, PA, USA, 2010.
28. *UNI EN 623-4:1994 Advanced Technical Ceramics—Monolithic Ceramics—General and Textural Properties—Part 4: Determination of Surface Roughness*; Ente Nazionale Italiano di Unificazione: Milano, Italy, 2005.
29. *UNI EN ISO 4287:2009 Geometrical Product Specifications (GPS)—Surface Texture: Profile Method—Terms, Definitions and Surface Texture Parameters*; International Standards Organization: Geneva, Switzerland, 2009.
30. *UNI EN 15886:2010 Conservation of Cultural Property—Test Methods—Colour Measurement of Surface*s; Ente Nazionale Italiano di Unificazione: Milano, Italy, 2010.
31. Tiago, F.; Wayne, R. The ImageJ User Guide 1.44; McGill university: Montreal, QC, Canada, 2011.
32. Wayne, R. *ImageJ*, v1.49; National Institutes of Health: Bethesda, MD, USA.